SIAM J. Applied Dynamical Systems
Vol. 18, No. 2, pp. 1143–1162

Analytical Description of Optimally Time-Dependent Modes for Reduced-Order Modeling of Transient Instabilities*

Antoine Blanchard† and Themistoklis P. Sapsis†

Abstract. The optimally time-dependent (OTD) modes form a time-evolving orthonormal basis that captures directions in phase space associated with transient and persistent instabilities. In the original formulation, the OTD modes are described by a set of coupled evolution equations that need to be solved along the trajectory of the system. For many applications where real-time estimation of the OTD modes is important, such as control or filtering, this is an expensive task. Here, we examine the low-dimensional structure of the OTD modes. In particular, we consider the case of slow-fast systems, and prove that OTD modes rapidly converge to a slow manifold, for which we derive an asymptotic expansion. The result is a parametric description of the OTD modes in terms of the system state in phase space. The analytical approximation of the OTD modes allows for their offline computation, making the whole framework suitable for real-time applications. In addition, we examine the accuracy of the slow-manifold approximation for systems in which there is no explicit time-scale separation. In this case, we show numerically that the asymptotic expansion of the OTD modes is still valid for regions of the phase space where strongly transient behavior is observed, and for which there is an implicit scale separation. We also find an analogy between the OTD modes and the Gram–Schmidt vectors (also known as orthogonal or backward Lyapunov vectors), and thereby establish new properties of the former. Several examples of low-dimensional systems are provided to illustrate the analytical formulation.

Key words. optimally time-dependent modes, Gram–Schmidt vectors, transient instabilities, slow-fast dynamics, invariant manifold

AMS subject classifications. 70K20, 70H33, 70K70

DOI. 10.1137/18M1212082

1. Introduction.

Prediction of transient instabilities and extreme events in high-dimensional systems has received considerable attention in recent years, as it has become one of the most prominent open problems in physics, engineering, and life sciences. Extreme events may be thought of as short-lived, large-amplitude bursting episodes interrupting quieter intervals of much longer duration (sometimes referred to as "maturation" [31, 2]) during which observables of a given trajectory remain relatively close to their mean values. The grand challenge is to produce reliable (ideally quantitative) indicators capable of signaling the imminence of an extreme event in a chaotic system. This is particularly critical in situations where extreme events have catastrophic consequences, as is the case with oceanic rogue waves [14] or, more generally, climate dynamics [9]. Situations in which extreme events are not synonymous

*Received by the editors September 6, 2018; accepted for publication by S. Shaw April 5, 2019; published electronically June 13, 2019.
http://www.siam.org/journals/siads/18-2/M121208.html
Funding: This work was supported by ARO grant W911NF-17-1-0306, AFOSR grant FA9550-16-1-0231, and ONR grant N00014-15-1-2381.
†Corresponding authors. Department of Mechanical Engineering, Massachusetts Institute of Technology, Cambridge, MA 02139 (ablancha@mit.edu, sapsis@mit.edu).

with dramatic outcomes have been considered as well, ranging from large-amplitude pulses in optical laser devices [36, 1] to intermittent fluctuations in turbulent models [19, 29, 12].

In a recent effort, Babaee and Sapsis [4] introduced a novel framework for predicting extreme events in high-dimensional dynamical systems. Their approach, based on a minimization principle, led to the concept of "optimally time-dependent (OTD) modes," a set of evolving orthonormal vectors that span the locally most unstable directions along a given trajectory, and therefore may serve as indicators for prediction of an upcoming extreme event. As discussed by Babaee and Sapsis [4] and Farazmand and Sapsis [16], the OTD modes provide a computationally stable tool to capture transient instabilities in a broad sense, including episodes of nonnormal growth, a task that poses great difficulty to conventional modal (eigenvalue-based) analysis. In a subsequent work, Babaee et al. [3] went beyond their original numerical investigations, and rigorously linked OTD modes and transient instabilities by showing that the OTD subspace rapidly converges to the subspace spanned by the most unstable eigendirections of the left Cauchy–Green tensor, that is, the directions associated with the largest finite-time Lyapunov exponents.

As noted in [3], the OTD modes are surmised to share fundamental features with existing measures of instability for chaotic systems. While connections between OTD modes, finite-time Lyapunov vectors [27], and dynamically orthogonal modes [34] have already been established, the question of whether OTD modes are related to Gram–Schmidt vectors (also known as orthogonal or backward Lyapunov vectors [5, 40]) and covariant Lyapunov vectors [20] remains to be explored. The latter two have been used primarily in the context of molecular dynamics in an attempt to quantify the rate of separation of two nearby trajectories in the phase space, which notion is intimately tied to thermodynamic irreversibility [25, 8, 23]. Gram–Schmidt vectors and covariant Lyapunov vectors have the interesting property that they converge at long times to well-defined bases that only depend on the state of the system in the phase space [22, 15]. A similar behavior has been seen for the OTD modes in various numerical experiments [4, 16, 3], and a rigorous proof that this is indeed the case would immediately open the door to a local (possibly approximate) analytical description of the OTD modes at any point in the phase space.

The present work aims to provide a definitive answer to this question. We consider a generic finite-dimensional autonomous system (which may be viewed as a projection of an infinite-dimensional autonomous system onto a finite-dimensional subset of complete functions), and find intimate connections between the OTD modes and the Gram–Schmidt vectors. This leads to the idea that at long times, the OTD modes can be expressed as a graph from the phase space to the OTD space, regardless of the prior history of the trajectory. With this in hand, we consider situations in which transient instabilities are associated with slow-fast dynamics and develop a method that provides analytical approximations for the OTD modes at every point in the phase space. We consider cases in which time-scale separation takes the form of a small parameter appearing explicitly in the equations of motion and cases in which it does not.

The remainder of the paper is structured as follows. We formulate the problem in section 2, investigate the relationship between OTD modes and Gram–Schmidt vectors in section 3, propose an analytical description of the OTD modes for slow-fast systems in section 4, extend the approach to general dynamical systems in section 5, and offer some conclusions in section 6.

2. Preliminaries.

2.1. Formulation of the problem.

We consider a generic n-dimensional autonomous dynamical system whose evolution in the phase space is governed by

$$\dot{\mathbf{z}} = \mathbf{F}(\mathbf{z}), \quad \mathbf{z} \in \mathbb{R}^n, \tag{2.1}$$

where the vector field $\mathbf{F} : \mathbb{R}^n \to \mathbb{R}^n$ is Lipschitz continuous, and the overdot denotes differentiation with respect to the time variable t. The solution of (2.1) for any initial condition $\mathbf{z}(t_0) = \mathbf{z}_0$ can be written as $\mathbf{z}(t; \mathbf{z}_0) = \phi_{t_0}^t(\mathbf{z}_0)$, where $\phi_{t_0}^t$ is the flow map in the phase space.

Infinitesimal perturbations about a given trajectory obey the variational equation

$$\dot{\mathbf{v}} = \mathbf{L}\mathbf{v}, \quad \mathbf{v} \in \mathbb{R}^n, \tag{2.2}$$

where $\mathbf{L} = \nabla_{\mathbf{z}}\mathbf{F}$ is a (generally) time-dependent linear operator. Stability of a reference orbit with respect to infinitesimal perturbations can be investigated by computing the Lyapunov spectrum of the trajectory. Lyapunov exponents quantify the rate at which an infinitesimal perturbation grows or decays along a trajectory, with positive (respectively, negative) values indicating growth (respectively, decay). Numerical computation of Lyapunov exponents generally requires integration of the variational equation over long time intervals, which poses significant issues related to numerical stability. This is because any r-dimensional subspace $\{\mathbf{v}_i(t_0)\}_{i=1}^r$ propagated by integrating the variational equation (2.2) rapidly collapses upon itself as a result of two confounding factors: (a) the magnitude of the individual members $\mathbf{v}_i(t)$ of the subspace grows or decays exponentially rapidly, and (b) the angle between each of them precipitously vanishes because each $\mathbf{v}_i(t)$ tends to align with the most unstable direction in the phase space, i.e., the first Lyapunov vector [39].

2.2. Review of the OTD modes.

The concept of OTD modes was first introduced in [4] in the form of a constrained minimization problem,

$$\arg\min_{\dot{\mathbf{u}}_i} \sum_{i=1}^{r} \|\dot{\mathbf{u}}_i - \mathbf{L}\mathbf{u}_i\|^2 \quad \text{subject to} \quad \langle \mathbf{u}_i, \mathbf{u}_j \rangle = \mathbf{I}_{r\times r}, \tag{2.3}$$

where $\langle \cdot, \cdot \rangle$ is a suitable inner product, $\|\cdot\|$ the induced norm, and $\mathbf{I}_{r\times r}$ the identity matrix of size r ($1 \le r \le n$). The vectors $\mathbf{u}_i(t)$ are the OTD modes, and they are by construction the best approximation of the linearized dynamics in the subspace that they span. As discussed in [4], the minimization problem (2.3) is equivalent to a set of coupled ordinary differential equations governing the evolution of each OTD mode. For the generic dynamical system (2.1) and an r-dimensional OTD subspace, the ith OTD mode obeys

$$\dot{\mathbf{u}}_i = \mathbf{L}\mathbf{u}_i - \sum_{k=1}^{r} \left(\langle \mathbf{L}\mathbf{u}_i, \mathbf{u}_k \rangle \mathbf{u}_k - \mathbf{\Phi}_{ik}\mathbf{u}_k \right), \tag{2.4}$$

where $\mathbf{\Phi}$ is a skew-symmetric, but otherwise arbitrary, tensor. As discussed in [4], the choice of $\mathbf{\Phi}$ does not affect the OTD subspace, since any two initially equivalent subspaces propagated with (2.4), each with a different choice of $\mathbf{\Phi}$, remain equivalent for all times. A natural

candidate for $\mathbf{\Phi}$ is the zero tensor, and this is what has been used in all of the studies on the subject [4, 16, 3]. However, choosing $\mathbf{\Phi} = \mathbf{0}$ leads to a fully coupled system of OTD equations, in that all r modes appear in each equation of (2.4). In contrast, choosing $\mathbf{\Phi}$ such that

$$\mathbf{\Phi}_{ik} = \begin{cases} -\langle \mathbf{L}\mathbf{u}_k, \mathbf{u}_i \rangle, & k < i, \\ 0, & k = i, \\ \langle \mathbf{L}\mathbf{u}_i, \mathbf{u}_k \rangle, & k > i, \end{cases} \tag{2.5}$$

leads to a system in which the equation for the ith mode depends only on the modes $\mathbf{u}_j$ with index $1 \leq j \leq i$. With this choice of $\mathbf{\Phi}$, the equation for the ith OTD mode reads

$$\dot{\mathbf{u}}_i = \mathbf{L}\mathbf{u}_i - \langle \mathbf{L}\mathbf{u}_i, \mathbf{u}_i \rangle \mathbf{u}_i - \sum_{k=1}^{i-1} \left(\langle \mathbf{L}\mathbf{u}_i, \mathbf{u}_k \rangle + \langle \mathbf{L}\mathbf{u}_k, \mathbf{u}_i \rangle \right) \mathbf{u}_k, \tag{2.6}$$

and the system assumes a lower triangular form, readily solvable by forward substitution. (We note that the summation index goes to $i-1$ in (2.6), rather than r as in (2.4).)

The OTD modes have the appealing property that they span the same flow-invariant subspace as the solutions $\{\mathbf{v}_i(t)\}_{i=1}^r$ of the variational equation (2.2), while preserving orthonormality for all times [4]. They thus provide a numerically stable means to computing transient features associated with finite-time instabilities. In particular, it has been shown that, under mildly restricting conditions, the OTD subspace converges exponentially fast to the eigenspace of the left Cauchy–Green tensor associated with transient instabilities [3]. Because of these properties, the OTD modes can serve as indicators for predicting upcoming bursts in a given trajectory [16]. This suggests possible connections to other methods capable of identifying unstable directions in the phase space, such as bred vectors [37], covariant Lyapunov vectors [20], or Gram–Schmidt vectors [5]. In what follows, we explore the relationship between OTD modes and Gram–Schmidt vectors.

3. Relationship between OTD modes and Gram–Schmidt vectors.

3.1. Review of the Gram–Schmidt vectors. The Gram–Schmidt (GS) vectors are generally computed by a method referred to as the "standard approach" [6, 35], which consists in evolving an initially orthonormal set of vectors with the variational equation (2.2), while periodically reorthonormalizing the integrated vectors using the GS algorithm. Formally, we begin by choosing r orthonormal vectors $\{\hat{\mathbf{e}}_i(t_0)\}_{i=1}^r$ as initial conditions for (2.2). These vectors are integrated forward in time until some prescribed instant $t = T$, which yields a new set of vectors $\{\mathbf{e}_i(T)\}_{i=1}^r$. The vectors $\mathbf{e}_i$ have lost their orthonormality in the process, so they are reorthonormalized by the classical GS algorithm as

$$\hat{\mathbf{e}}_i(T) = \frac{\mathbf{e}_i(T) - \sum_{k=1}^{i-1} \langle \hat{\mathbf{e}}_k(T), \mathbf{e}_i(T) \rangle \hat{\mathbf{e}}_k(T)}{\left\| \mathbf{e}_i(T) - \sum_{k=1}^{i-1} \langle \hat{\mathbf{e}}_k(T), \mathbf{e}_i(T) \rangle \hat{\mathbf{e}}_k(T) \right\|}. \tag{3.1}$$

The procedure is repeated using $\hat{\mathbf{e}}_i(T)$ as initial conditions for (2.2). The reorthonormalization time T must be chosen small enough so as to not compromise the accuracy of the GS algorithm and avoid blowup of the solution.

Of the many results that have been established about GS vectors, we review a few relevant to the present work. First, the first GS vector tends to seek the most rapidly growing direction in the tangent space. The second GS vector is not free to seek the most rapidly growing direction, nor the second most rapidly growing direction, because the second GS vector is constrained to live in the orthogonal complement of the first GS vector. However, the subspace spanned by the first two GS vectors continually seeks the two-dimensional subspace that is most rapidly growing [39].

Second, for ergodic systems, the GS vectors converge to a well-defined basis that depends only on the state $\mathbf{z}$ in the phase space, and not on the history of the trajectory [22, 15]. More precisely, the GS vectors converge exponentially rapidly to the eigenvectors of the inverse-time Oseledec matrix [28, 20] (sometimes referred to as the far-past operator [26]), defined as

$$\mathbf{\Theta}(t) = \lim_{t_1 \to -\infty} \left[\mathbf{M}(t_1, t)^{-T} \mathbf{M}(t_1, t)^{-1}\right]^{1/2(t-t_1)}, \tag{3.2}$$

where $\mathbf{M}(t_1, t)$ is the state-transition matrix associated with the variational equation (2.2) over the time interval $[t_1, t]$. We also mention that the GS vectors are not covariant with the linearized dynamics; that is, the GS vectors at a given point in the phase space are not mapped by the linearized dynamics (2.2) into the GS vectors at the forward image of that point (they do, however, span the same subspace) [21]. An immediate consequence is that the GS vectors are not invariant with respect to the time-reversed dynamics. This is in contrast to covariant Lyapunov vectors, whose definition, properties, and relationship to GS vectors are discussed in [21, 40, 7].

3.2. Equivalence between GS vectors and OTD modes. Here, we show that the GS vectors and the OTD modes coincide in the limit $T \to 0$, that is, when the GS vectors are *continuously* orthonormalized.

We first consider an orthonormal basis $\{\hat{\mathbf{e}}_i(t_0)\}_{i=1}^r$ of an r-dimensional subspace in $\mathbb{R}^n$. We advance each of the $\hat{\mathbf{e}}_i(t_0)$ with the variational equation (2.2) over an infinitesimal time interval δt, from t_0 to $t_0 + \delta t$. To first order, we have

$$\mathbf{e}_i(t_0 + \delta t) = \hat{\mathbf{e}}_i(t_0) + \mathbf{L}(t_0)\hat{\mathbf{e}}_i(t_0)\delta t + \mathcal{O}(\delta t^2). \tag{3.3}$$

As discussed in subsection 3.1, the $\mathbf{e}_i$ are no longer orthonormal at $t_0 + \delta t$. We therefore invoke the GS algorithm to reorthonormalize them.

The first GS vector at $t_0 + \delta t$ is given by

$$\hat{\mathbf{e}}_1(t_0 + \delta t) = \frac{\mathbf{e}_1(t_0 + \delta t)}{\|\mathbf{e}_1(t_0 + \delta t)\|} = \frac{\hat{\mathbf{e}}_1(t_0) + \mathbf{L}(t_0)\hat{\mathbf{e}}_1(t_0)\delta t + \mathcal{O}(\delta t^2)}{\|\hat{\mathbf{e}}_1(t_0) + \mathbf{L}(t_0)\hat{\mathbf{e}}_1(t_0)\delta t + \mathcal{O}(\delta t^2)\|}. \tag{3.4}$$

Taylor expanding the norm and recognizing that $\|\hat{\mathbf{e}}_i(t_0)\| = 1$, we obtain

$$\left\|\hat{\mathbf{e}}_1(t_0) + \mathbf{L}(t_0)\hat{\mathbf{e}}_1(t_0)\delta t + \mathcal{O}(\delta t^2)\right\| = 1 + \langle \mathbf{L}(t_0)\hat{\mathbf{e}}_1(t_0), \hat{\mathbf{e}}_1(t_0)\rangle \delta t + \mathcal{O}(\delta t^2), \tag{3.5}$$

which, upon substitution into (3.4), leads to

$$\hat{\mathbf{e}}_1(t_0+\delta t) = \hat{\mathbf{e}}_1(t_0) + \mathbf{L}(t_0)\hat{\mathbf{e}}_1(t_0)\delta t - \langle \mathbf{L}(t_0)\hat{\mathbf{e}}_1(t_0), \hat{\mathbf{e}}_1(t_0)\rangle \hat{\mathbf{e}}_1(t_0)\delta t + \mathcal{O}(\delta t^2). \tag{3.6}$$

Proceeding to the limit $\delta t \to 0$ gives

$$\dot{\hat{\mathbf{e}}}_1 = \mathbf{L}\hat{\mathbf{e}}_1 - \langle \mathbf{L}\hat{\mathbf{e}}_1, \hat{\mathbf{e}}_1\rangle \hat{\mathbf{e}}_1, \tag{3.7}$$

which is identical to the first of (2.6).

Similarly, the second GS vector is written as

$$\hat{\mathbf{e}}_2(t_0+\delta t) = \frac{\mathbf{e}_2(t_0+\delta t) - [\langle \mathbf{e}_2(t_0+\delta t), \hat{\mathbf{e}}_1(t_0+\delta t)\rangle]\, \hat{\mathbf{e}}_1(t_0+\delta t)}{\|\mathbf{e}_2(t_0+\delta t) - [\langle \mathbf{e}_2(t_0+\delta t), \hat{\mathbf{e}}_1(t_0+\delta t)\rangle]\, \hat{\mathbf{e}}_1(t_0+\delta t)\|}. \tag{3.8}$$

The above can be expanded as

$$\hat{\mathbf{e}}_2(t_0+\delta t) = \frac{\hat{\mathbf{e}}_2 + \mathbf{L}\hat{\mathbf{e}}_2\delta t - \langle \mathbf{L}\hat{\mathbf{e}}_1, \hat{\mathbf{e}}_2\rangle \hat{\mathbf{e}}_1\delta t - \langle \mathbf{L}\hat{\mathbf{e}}_2, \hat{\mathbf{e}}_1\rangle \hat{\mathbf{e}}_1\delta t + \mathcal{O}(\delta t^2)}{1 + \langle \mathbf{L}\hat{\mathbf{e}}_2, \hat{\mathbf{e}}_2\rangle \delta t + \mathcal{O}(\delta t^2)}, \tag{3.9}$$

where all of the quantities on the right-hand side are evaluated at time t_0. Taking the limit $\delta t \to 0$ as before, we obtain

$$\dot{\hat{\mathbf{e}}}_2 = \mathbf{L}\hat{\mathbf{e}}_2 - \langle \mathbf{L}\hat{\mathbf{e}}_2, \hat{\mathbf{e}}_2\rangle \hat{\mathbf{e}}_2 - (\langle \mathbf{L}\hat{\mathbf{e}}_2, \hat{\mathbf{e}}_1\rangle + \langle \mathbf{L}\hat{\mathbf{e}}_1, \hat{\mathbf{e}}_2\rangle)\, \hat{\mathbf{e}}_1 \tag{3.10}$$

as the differential equation for $\hat{\mathbf{e}}_2$. This equation is identical to the second of (2.6).

Proceeding in this manner, we show by induction that the ith GS vector $\hat{\mathbf{e}}_i$ obeys

$$\dot{\hat{\mathbf{e}}}_i = \mathbf{L}\hat{\mathbf{e}}_i - \langle \mathbf{L}\hat{\mathbf{e}}_i, \hat{\mathbf{e}}_i\rangle \hat{\mathbf{e}}_i - \sum_{k=1}^{i-1} (\langle \mathbf{L}\hat{\mathbf{e}}_i, \hat{\mathbf{e}}_k\rangle + \langle \mathbf{L}\hat{\mathbf{e}}_k, \hat{\mathbf{e}}_i\rangle)\, \hat{\mathbf{e}}_k, \tag{3.11}$$

which is identical to (2.6). This shows that the GS vectors and the OTD modes obey the same governing equations, and thus correspond to the same mathematical object. (This result holds regardless of the choice of norm, and carries over to infinite-dimensional spaces.) A direct consequence of this equivalence is that GS vectors and OTD modes share the same mathematical properties. In particular, all of the properties pertaining to the GS vectors that were stated in subsection 3.1 trivially apply to the OTD modes. To these, we add that the OTD modes (i.e., continuously orthonormalized GS vectors) can be used as a numerically stable tool to compute infinite-horizon Lyapunov exponents. The leading one-dimensional Lyapunov exponents are given by

$$\lambda_i = \lim_{t\to\infty} \frac{1}{t-t_0} \int_{t_0}^{t} \langle \mathbf{u}_i, \mathbf{L}\mathbf{u}_i\rangle \, \mathrm{d}\tau, \tag{3.12}$$

which is nothing more than the time average of the diagonal Lagrange multipliers $\langle \mathbf{u}_i, \mathbf{L}\mathbf{u}_i\rangle$ [22, 38, 24].

Another consequence of this equivalence is that the GS vectors, when continuously orthonormalized, are solutions of the minimization problem (2.3) from which the OTD equations (2.6) were derived. The GS vectors can therefore be viewed as best approximating the lin-

earized dynamics in the subspace that they span. It is not obvious that this conclusion could have been readily drawn from the GS "standard approach." We note, however, that others had previously hinted at the idea of incorporating constraints in the variational equations to compute Lyapunov exponents [32].

We finally mention that the OTD modes have been successfully used to construct dynamically consistent reduced-order models of the linearized dynamics. This was done by projecting $\mathbf{L}$ onto an r-dimensional OTD subspace, which yielded a *reduced linear operator* [16]. This procedure is greatly advantageous in high-dimensional systems as it allows tracking of unstable directions at much lower computational cost than otherwise required by integration of the full-order system. To the best of our knowledge, this idea had not been considered in the context of GS vectors until now.

In all that follows, we make no distinction between GS vectors and OTD modes.

4. Analytical expansion of OTD modes associated with slow-fast dynamics. An importance consequence of the equivalence between GS vectors and OTD modes is the existence of a graph $\mathbf{z} \mapsto \mathbf{u}_i(\mathbf{z})$ that follows from the fact that the GS vectors, at long times, only depend on the point of the attractor where they are computed [15]. In this section, we propose an analytical description of this graph in cases where the vector field $\mathbf{F}$ can be written in terms of slow and fast variables, with the ratio of the slow and fast time scales being governed by a small parameter ε that explicitly appears in the governing equations. (Here, and in all that follows, we use the standard inner product on $\mathbb{R}^n$.)

4.1. Formulation of the slow-fast problem. We begin by assuming that (2.1) exhibits slow-fast dynamics, and can be decomposed in terms of slow and fast variables as

$$\varepsilon \dot{\mathbf{x}} = \mathbf{f}(\mathbf{x}, \mathbf{y}; \varepsilon), \tag{4.1a}$$

$$\dot{\mathbf{y}} = \mathbf{g}(\mathbf{x}, \mathbf{y}; \varepsilon), \tag{4.1b}$$

where $\mathbf{x} \in \mathbb{R}^p$ and $\mathbf{y} \in \mathbb{R}^q$ are the fast and slow variables, respectively, $\varepsilon \in \mathbb{R}^+$ is a small parameter, and $p+q=n$. We assume that the vector fields $\mathbf{f}$ and $\mathbf{g}$ are equally smooth as the original vector field $\mathbf{F}$. It is possible to convert (4.1a) and (4.1b) into a regular perturbation problem by introducing the fast time scale $\tau = t/\varepsilon$, which leads to

$$\mathbf{x}' = \mathbf{f}(\mathbf{x}, \mathbf{y}; \varepsilon), \tag{4.2a}$$

$$\mathbf{y}' = \varepsilon \mathbf{g}(\mathbf{x}, \mathbf{y}; \varepsilon), \tag{4.2b}$$

where prime denotes differentiation with respect to τ. In contrast to (4.1a) and (4.1b), the fast-time system is amenable to regular perturbation theory. Invariant manifold theory guarantees the existence of a limiting slow manifold $\mathcal{W}_0$ corresponding to the fixed points of (4.2a) in the limit $\varepsilon \to 0$. It is given by

$$\mathcal{W}_0 = \{(\mathbf{x}, \mathbf{y}) \,|\, \mathbf{f}(\mathbf{x}, \mathbf{y}; 0) = \mathbf{0}\}. \tag{4.3}$$

We further assume that the vector fields $\mathbf{f}$ and $\mathbf{g}$ are sufficiently smooth functions of ε and, therefore, admit expansions of the form

$$\mathbf{b}(\mathbf{x}, \mathbf{y}; \varepsilon) = \sum_{k=0}^{\infty} \varepsilon^k \left. \frac{\partial^{(k)} \mathbf{b}(\mathbf{x}, \mathbf{y}; \varepsilon)}{\partial \varepsilon^{(k)}} \right|_{\varepsilon=0} \equiv \sum_{k=0}^{\infty} \varepsilon^k \mathbf{b}_k(\mathbf{x}, \mathbf{y}), \tag{4.4}$$

where $\mathbf{b}$ is a placeholder for $\mathbf{f}$ and $\mathbf{g}$. It should be clear that the manifold equation (4.3) is equivalent to $\mathbf{f}_0(\mathbf{x},\mathbf{y}) = \mathbf{0}$. Fenichel's theorem states that for $\varepsilon > 0$, there exists a slow invariant manifold (SIM) given by

$$\mathcal{W}_\varepsilon = \{(\mathbf{x},\mathbf{y}) \,|\, \mathbf{x} = \bar{\mathbf{x}}(\mathbf{y};\varepsilon)\}, \tag{4.5}$$

where $\bar{\mathbf{x}}(\mathbf{y};\varepsilon)$ is a smooth graph over the slow variable $\mathbf{y}$ [18]. The graph $\bar{\mathbf{x}}$ smoothly deforms with ε, and satisfies $\mathbf{x} = \bar{\mathbf{x}}(\mathbf{y};0) \Leftrightarrow \mathbf{f}_0(\mathbf{x},\mathbf{y}) = \mathbf{0}$, a consequence of the implicit-function theorem. An analytical expression for $\mathcal{W}_\varepsilon$ can be derived by rewriting (4.1a) as

$$\varepsilon \nabla_{\mathbf{y}} \bar{\mathbf{x}}(\mathbf{y};\varepsilon)\, \mathbf{g}(\bar{\mathbf{x}}(\mathbf{y};\varepsilon),\mathbf{y};\varepsilon) = \mathbf{f}(\bar{\mathbf{x}}(\mathbf{y};\varepsilon),\mathbf{y};\varepsilon), \tag{4.6}$$

and invoking the approximation theorem for SIMs [17, 33]. The latter states that an approximation of the graph $\bar{\mathbf{x}}$ can be constructed as a power series $\bar{\mathbf{x}}(\mathbf{y};\varepsilon) = \bar{\mathbf{x}}_0(\mathbf{y}) + \varepsilon \bar{\mathbf{x}}_1(\mathbf{y}) + \cdots$ that satisfies (4.6) at each order of approximation.

We now turn to the dynamics of the system resulting from linearizing (4.2a) and (4.2b) around the trajectory, which obeys

$$\begin{bmatrix} \mathbf{v}' \\ \mathbf{w}' \end{bmatrix} = \begin{bmatrix} \nabla_{\mathbf{x}} \mathbf{f}(\mathbf{x},\mathbf{y};\varepsilon) & \nabla_{\mathbf{y}} \mathbf{f}(\mathbf{x},\mathbf{y};\varepsilon) \\ \varepsilon \nabla_{\mathbf{x}} \mathbf{g}(\mathbf{x},\mathbf{y};\varepsilon) & \varepsilon \nabla_{\mathbf{y}} \mathbf{g}(\mathbf{x},\mathbf{y};\varepsilon) \end{bmatrix} \begin{bmatrix} \mathbf{v} \\ \mathbf{w} \end{bmatrix} \equiv \mathbf{J} \begin{bmatrix} \mathbf{v} \\ \mathbf{w} \end{bmatrix}, \tag{4.7}$$

and likewise admits a limiting invariant manifold given by

$$\nabla_{\mathbf{x}} \mathbf{f}_0(\mathbf{x},\mathbf{y})\mathbf{v} + \nabla_{\mathbf{y}} \mathbf{f}_0(\mathbf{x},\mathbf{y})\mathbf{w} = \mathbf{0}. \tag{4.8}$$

The Jacobian $\mathbf{J}$ can be expanded as

$$\mathbf{J} = \begin{bmatrix} \nabla_{\mathbf{x}} \mathbf{f}_0(\mathbf{x},\mathbf{y}) & \nabla_{\mathbf{y}} \mathbf{f}_0(\mathbf{x},\mathbf{y}) \\ \mathbf{0} & \mathbf{0} \end{bmatrix} + \varepsilon \begin{bmatrix} \nabla_{\mathbf{x}} \mathbf{f}_1(\mathbf{x},\mathbf{y}) & \nabla_{\mathbf{y}} \mathbf{f}_1(\mathbf{x},\mathbf{y}) \\ \nabla_{\mathbf{x}} \mathbf{g}_0(\mathbf{x},\mathbf{y}) & \nabla_{\mathbf{y}} \mathbf{g}_0(\mathbf{x},\mathbf{y}) \end{bmatrix} + \mathcal{O}(\varepsilon^2) \tag{4.9}$$

or, equivalently, $\mathbf{J} = \mathbf{J}_0 + \varepsilon \mathbf{J}_1 + \mathcal{O}(\varepsilon^2)$. The operator $\mathbf{J}_0$ corresponds to the zeroth-order approximation of the original linearized operator $\mathbf{J}$. We note that $\mathbf{J}_0$ has a nontrivial kernel whose dimension equals the number of slow variables (that is, $\dim(\operatorname{Ker} \mathbf{J}_0) = q$). Thus, $\mathbf{J}_0$ has q trivial eigenvectors associated with eigenvalue 0, and p nontrivial eigenvectors associated with nonzero eigenvalues. Since $\mathbf{J}_0$ is an upper-triangular block matrix, the nontrivial eigenvectors (and associated eigenvalues) coincide with those of $\nabla_{\mathbf{x}} \mathbf{f}_0(\mathbf{x},\mathbf{y})$. In what follows, we assume that the manifold defined by (4.3) is asymptotically stable, so that the eigenvalues of $\nabla_{\mathbf{x}} \mathbf{f}_0(\mathbf{x},\mathbf{y})$ all have negative real parts. The center-manifold theorem then guarantees that $\mathcal{W}_\varepsilon$ is locally attractive [10].

We note that the eigenvalue problem $\mathbf{J}\mathbf{r} = \lambda \mathbf{r}$ associated with the slow-fast variational equations (4.7) can be rewritten as a series of subproblems using asymptotic expansions in ε for $\mathbf{r}$ and λ. Letting $\mathbf{r} = \mathbf{r}_0 + \varepsilon \mathbf{r}_1 + \cdots$ and $\lambda = \lambda_0 + \varepsilon \lambda_1 + \cdots$, we have

$$\mathbf{J}_0 \mathbf{r}_0 = \lambda_0 \mathbf{r}_0, \tag{4.10a}$$

$$\mathbf{J}_1 \mathbf{r}_0 + \mathbf{J}_0 \mathbf{r}_1 = \lambda_0 \mathbf{r}_1 + \lambda_1 \mathbf{r}_0 \tag{4.10b}$$

at $\mathcal{O}(1)$ and $\mathcal{O}(\varepsilon)$, respectively. This leads to

$$\lambda = \mathbf{r}_0^T \mathbf{J}_0 \mathbf{r}_0 + \mathcal{O}(\varepsilon), \tag{4.11}$$

which shows that any eigenvalue of $\mathbf{J}$ associated with an eigenvector $\mathbf{r}$ such that $\mathbf{r}_0 \in \operatorname{Ker} \mathbf{J}_0$ scales like $\mathcal{O}(\varepsilon)$.

4.2. Slow invariant manifold for the OTD modes. We now examine the OTD equations, and propose a manifold approach similar to the classical technique reviewed in subsection 4.1. The goal is to show that for a trajectory $(\mathbf{x}, \mathbf{y})$ evolving on $\mathcal{W}_\varepsilon$, the OTD modes associated with that trajectory evolve on a SIM of their own and, therefore, can be written as a power series in ε whose coefficients depend only on the state $(\mathbf{x}, \mathbf{y})$ of the dynamical system. In other words, we wish to find a graph from the physical space $(\mathbf{x}, \mathbf{y})$ to the OTD space in the form of an asymptotic expansion in terms of the small parameter ε.

Here, we consider the case of a one-dimensional OTD subspace ($r = 1$). This does not restrict the scope of the analysis because any OTD mode can be computed in a fashion similar to the below, provided that the OTD modes with lower indices have been computed. For the slow-fast system (4.1a) and (4.1b), the first OTD mode $\mathbf{u}_1$ obeys

$$\varepsilon \dot{\mathbf{u}}_1 = \mathbf{J}\mathbf{u}_1 - \mathbf{u}_1(\mathbf{u}_1^T \mathbf{J}\mathbf{u}_1) \tag{4.12}$$

at the slow time scale, and

$$\mathbf{u}_1' = \mathbf{J}\mathbf{u}_1 - \mathbf{u}_1(\mathbf{u}_1^T \mathbf{J}\mathbf{u}_1) \tag{4.13}$$

at the fast time scale. We note that in (4.12), there is no slow-fast partition of the coordinates for $\mathbf{u}_1$ because the linearized operator $\mathbf{J}$ appears in a bilinear form over $\mathbf{u}_1$. We discard the numeral subscript for clarity, and manipulate (4.12) to obtain

$$\varepsilon(\nabla_{\mathbf{x}}\mathbf{u}\,\dot{\mathbf{x}} + \nabla_{\mathbf{y}}\mathbf{u}\,\dot{\mathbf{y}}) = (\mathbf{I} - \mathbf{u}\mathbf{u}^T)\mathbf{J}\mathbf{u}, \tag{4.14}$$

where we have invoked the chain rule on $\dot{\mathbf{u}}$. Using (4.1a) and (4.1b), the above leads to

$$\nabla_{\mathbf{x}}\mathbf{u}\,\mathbf{f}(\mathbf{x}, \mathbf{y}; \varepsilon) + \varepsilon \nabla_{\mathbf{y}}\mathbf{u}\,\mathbf{g}(\mathbf{x}, \mathbf{y}; \varepsilon) = (\mathbf{I} - \mathbf{u}\mathbf{u}^T)\mathbf{J}\mathbf{u}. \tag{4.15}$$

Assuming that appropriate smoothness conditions are satisfied, we introduce the asymptotic expansion $\mathbf{u} = \mathbf{u}^{(0)} + \varepsilon\mathbf{u}^{(1)} + \cdots$, which we substitute in (4.15) to obtain a hierarchy of subproblems at each order of approximation in ε. We mention at this point that the normalization property of $\mathbf{u}$ carries over to the above expansion, but only up to the highest order considered. In other words, we require that $\|\mathbf{u}^{(0)} + \cdots + \varepsilon^k \mathbf{u}^{(k)}\| = 1 + \mathcal{O}(\varepsilon^{k+1})$. In particular, this means that $\mathbf{u}^{(0)} \perp \mathbf{u}^{(1)}$, since

$$\|\mathbf{u}^{(0)} + \varepsilon\mathbf{u}^{(1)}\| = \|\mathbf{u}^{(0)}\| + \varepsilon \frac{\langle \mathbf{u}^{(0)}, \mathbf{u}^{(1)} \rangle}{\|\mathbf{u}^{(0)}\|} + \mathcal{O}(\varepsilon^2). \tag{4.16}$$

The $\mathcal{O}(1)$ subproblem reads

$$\nabla_{\mathbf{x}}\mathbf{u}^{(0)}\mathbf{f}_0(\mathbf{x}, \mathbf{y}) = (\mathbf{I} - \mathbf{u}^{(0)}\mathbf{u}^{(0)T})\mathbf{J}_0\mathbf{u}^{(0)}. \tag{4.17}$$

Because (4.3) demands that $\mathbf{f}_0(\mathbf{x}, \mathbf{y}) = 0$, we immediately obtain the equation defining the limiting invariant manifold for the OTD mode,

$$(\mathbf{I} - \mathbf{u}^{(0)}\mathbf{u}^{(0)T})\mathbf{J}_0\mathbf{u}^{(0)} = \mathbf{0}. \tag{4.18}$$

The limiting invariant manifold coincides with the fixed points of the fast-scale equation (4.13). It is defined as the set of solutions of a nonlinear algebraic equation in $\mathbf{u}^{(0)}$, in which dependence on the state variables $(\mathbf{x}, \mathbf{y})$ appears through the linear operator $\mathbf{J}_0$. By virtue of the implicit-function theorem, we conclude that $\mathbf{u}^{(0)}$ can be expressed as a graph over the state variables $(\mathbf{x}, \mathbf{y})$, and that this graph must solve the $\mathcal{O}(1)$ subproblem (4.18). Consistent with [4], the limiting invariant manifold comprises any normalized $\mathbf{u}^{(0)} \in \operatorname{Ker} \mathbf{J}_0$, as well as any normalized nontrivial eigenvector of $\mathbf{J}_0$.

We proceed to consider the $\mathcal{O}(\varepsilon)$ subproblem, which is given by

$$\begin{aligned} \nabla_{\mathbf{x}} \mathbf{u}^{(0)} \mathbf{f}_1(\mathbf{x}, \mathbf{y}) + \nabla_{\mathbf{y}} \mathbf{u}^{(0)} \mathbf{g}_0(\mathbf{x}, \mathbf{y}) = (\mathbf{I} - \mathbf{u}^{(0)} \mathbf{u}^{(0)T})(\mathbf{J}_0 \mathbf{u}^{(1)} + \mathbf{J}_1 \mathbf{u}^{(0)}) \\ - (\mathbf{u}^{(1)} \mathbf{u}^{(0)T} + \mathbf{u}^{(0)} \mathbf{u}^{(1)T}) \mathbf{J}_0 \mathbf{u}^{(0)}. \end{aligned} \tag{4.19}$$

We note that the $\mathcal{O}(\varepsilon)$ subproblem is linear in $\mathbf{u}^{(1)}$. (In fact, it is easy to see that all of the $\mathcal{O}(\varepsilon^k)$ subproblems (for $k > 0$) are linear in $\mathbf{u}^{(k)}$.) Recognizing that $\mathbf{u}^{(0)}$ must be orthogonal to $\mathbf{u}^{(1)}$, the above can be simplified as

$$\nabla \mathbf{u}^{(0)} \, \mathbf{h}_1(\mathbf{x}, \mathbf{y}) = (\mathbf{I} - \mathbf{u}^{(0)} \mathbf{u}^{(0)T})(\mathbf{J}_0 \mathbf{u}^{(1)} + \mathbf{J}_1 \mathbf{u}^{(0)}) - \mathbf{u}^{(1)} \mathbf{u}^{(0)T} \mathbf{J}_0 \mathbf{u}^{(0)}, \tag{4.20}$$

where we have introduced the compact notation

$$\nabla \mathbf{u}^{(0)} = \begin{bmatrix} \nabla_{\mathbf{x}} \mathbf{u}^{(0)} & \nabla_{\mathbf{y}} \mathbf{u}^{(0)} \end{bmatrix}, \tag{4.21a}$$

$$\mathbf{h}_1(\mathbf{x}, \mathbf{y}) = \begin{bmatrix} \mathbf{f}_1(\mathbf{x}, \mathbf{y}) & \mathbf{g}_0(\mathbf{x}, \mathbf{y}) \end{bmatrix}^T. \tag{4.21b}$$

For (4.20) to have solutions, the Fredholm alternative requires that

$$\nabla \mathbf{u}^{(0)} \, \mathbf{h}_1(\mathbf{x}, \mathbf{y}) - (\mathbf{I} - \mathbf{u}^{(0)} \mathbf{u}^{(0)T}) \mathbf{J}_1 \mathbf{u}^{(0)} \perp \operatorname{Ker} (\mathbf{I} - \mathbf{u}^{(0)} \mathbf{u}^{(0)T}) \mathbf{J}_0 - (\mathbf{u}^{(0)T} \mathbf{J}_0 \mathbf{u}^{(0)}) \mathbf{I}. \tag{4.22}$$

This condition provides m constraint equations, where m is the dimension of the kernel on the right-hand side of (4.22). We note without proof that $m = 0$ when $\mathbf{u}^{(0)}$ is a nontrivial eigenvector of $\mathbf{J}_0$, and $m = q$ when $\mathbf{u}^{(0)} \in \operatorname{Ker} \mathbf{J}_0$. This means that if $\mathbf{u}^{(0)}$ is a nontrivial eigenvector of $\mathbf{J}_0$, then (4.20) is a well-posed problem and admits a unique (nonvanishing) solution. On the other hand, if $\mathbf{u}^{(0)} \in \operatorname{Ker} \mathbf{J}_0$, then $\mathbf{u}^{(0)}$ can be written as a linear combination of q basis vectors of $\operatorname{Ker} \mathbf{J}_0$, and the unknown basis coefficients can be determined using the q constraint equations from (4.22). Once the latter has been enforced, one can solve (4.20) for $\mathbf{u}^{(1)}$, and proceed to the next order in ε.

It is straightforward to show that the asymptotic OTD formulation is consistent with the results of Babaee and Sapsis [4], who showed that for steady dynamics the OTD subspace asymptotically coincides with the subspace spanned by the most unstable eigenvectors of the linearized operator. With the notation introduced above, this means that $\mathbf{u}^{(i)} = \mathbf{r}_i$. We illustrate this point below.

4.3. Examples. We apply the approach proposed in subsection 4.2 to two low-dimensional systems featuring slow-fast dynamics. We note that low dimensionality is a prerequisite for the SIM approach to be analytically tractable. (Systems with dimensionality greater than three must generally be treated numerically.)

4.3.1. Steady linear dynamics. We first consider the slow-fast system

$$\varepsilon \dot{x} = -x + y, \tag{4.23a}$$

$$\dot{y} = x/2 - y, \tag{4.23b}$$

for which

$$\mathbf{J} = \begin{bmatrix} -1 & 1 \\ \varepsilon/2 & -\varepsilon \end{bmatrix}. \tag{4.24}$$

The linearized operator $\mathbf{J}$ is steady and nonnormal, leading initially to rapid growth of the solution over short times, followed by a slow decay to steady state. The eigenvectors of $\mathbf{J}$ are given by

$$\mathbf{r}_- = \begin{bmatrix} -1 + (\varepsilon^2/8) + \mathcal{O}(\varepsilon^3) \\ (\varepsilon/2) + (\varepsilon^2/4) + \mathcal{O}(\varepsilon^3) \end{bmatrix}, \tag{4.25a}$$

$$\mathbf{r}_+ = (1/\sqrt{2}) \begin{bmatrix} 1 + (\varepsilon/4) - (3\varepsilon^2/32) + \mathcal{O}(\varepsilon^3) \\ 1 - (\varepsilon/4) + (\varepsilon^2/32) + \mathcal{O}(\varepsilon^3) \end{bmatrix}, \tag{4.25b}$$

associated with $\lambda_- = -1 - (\varepsilon/2) - (\varepsilon^2/4) + \mathcal{O}(\varepsilon^3)$ and $\lambda_+ = -(\varepsilon/2) + (\varepsilon^2/4) + \mathcal{O}(\varepsilon^3)$, respectively. (It should be clear that $\lambda_+ > \lambda_-$ for any $\varepsilon \in \mathbb{R}^+$.) We recall that for linear time-invariant systems, the OTD subspace asymptotically coincides with the subspace spanned by the most unstable eigenvectors of the linear operator [4]. In what follows, we show that the manifold approach developed in subsection 4.2 recovers this feature.

We begin by solving the $\mathcal{O}(1)$ subproblem $(\mathbf{I} - \mathbf{u}^{(0)}\mathbf{u}^{(0)T})\mathbf{J}_0\mathbf{u}^{(0)} = 0$, where

$$\mathbf{J}_0 = \begin{bmatrix} -1 & 1 \\ 0 & 0 \end{bmatrix}. \tag{4.26}$$

We find two solutions in the limiting invariant manifold,

$$\mathbf{u}^{(0)} = \begin{bmatrix} -1 & 0 \end{bmatrix}^T \in (\operatorname{Ker} \mathbf{J}_0)^{\mathrm{c}}, \tag{4.27a}$$

$$\mathbf{u}^{(0)} = \alpha \begin{bmatrix} 1 & 1 \end{bmatrix}^T \in \operatorname{Ker} \mathbf{J}_0, \tag{4.27b}$$

where α is a factor yet to be determined, and the superscript "c" denotes the complementary set. We note that the solution belonging to $\operatorname{Ker} \mathbf{J}_0$ is determined only up to a multiplicative factor as a result of the singular nature of $\mathbf{J}_0$. Because the linear operator is steady, the unknown multiplicative factor α does not depend on the state variables x and y. Another way to see this is to invoke the implicit-function theorem in the $\mathcal{O}(1)$ subproblem since the latter does not depend on the state variables. Here, we select α by simply requiring that $\|\mathbf{u}^{(0)}\| = 1$.

As discussed in subsection 4.2, the higher-order subproblems for the solution in $(\operatorname{Ker} \mathbf{J}_0)^{\mathrm{c}}$ admit a unique solution. The $\mathcal{O}(\varepsilon)$ and $\mathcal{O}(\varepsilon^2)$ subproblems yield

$$\mathbf{u}^{(1)} = \begin{bmatrix} 0 & 1/2 \end{bmatrix}^T, \tag{4.28a}$$

$$\mathbf{u}^{(2)} = \begin{bmatrix} 1/8 & 1/4 \end{bmatrix}^T. \tag{4.28b}$$

Collecting the expansion coefficients from (4.27a), (4.28a), and (4.28b), we obtain a solution that coincides with $\mathbf{r}_-$. We note that, consistent with (4.11), the OTD solution with $\mathbf{u}^{(0)} \in (\operatorname{Ker}\mathbf{J}_0)^{\mathrm{c}}$ is associated with the least unstable $\mathcal{O}(1)$ eigenvalue.

We now proceed with (4.27b), for which normalization requires that $\alpha = 1/\sqrt{2}$. The $\mathcal{O}(\varepsilon)$ subproblem has a line of solutions,

$$\mathbf{u}^{(1)} = \begin{bmatrix}\beta & \beta - (\sqrt{2}/4)\end{bmatrix}^T, \tag{4.29}$$

where β is an undetermined factor, which is selected so that $\|\mathbf{u}^{(0)} + \varepsilon\mathbf{u}^{(1)}\| = \mathcal{O}(\varepsilon^2)$ or, equivalently, $\mathbf{u}^{(0)} \perp \mathbf{u}^{(1)}$. This gives

$$\mathbf{u}^{(1)} = 1/(4\sqrt{2})\begin{bmatrix}1 & -1\end{bmatrix}^T. \tag{4.30}$$

The $\mathcal{O}(\varepsilon^2)$ subproblem also has a line of solutions, which we restrict by requiring that $\|\mathbf{u}^{(0)} + \varepsilon\mathbf{u}^{(1)} + \varepsilon^2\mathbf{u}^{(2)}\| = \mathcal{O}(\varepsilon^3)$, giving

$$\mathbf{u}^{(2)} = 1/(\sqrt{2})\begin{bmatrix}-3/32 & 1/32\end{bmatrix}^T. \tag{4.31}$$

Proceeding in a similar fashion with higher orders, we conclude that the approximation of the OTD mode for which $\mathbf{u}^{(0)} \in \operatorname{Ker}\mathbf{J}_0$ coincides with $\mathbf{r}_+$.

We note that strictly speaking, the undetermined factors α and β should be computed with the Fredholm alternative, as prescribed in subsection 4.2. The above example suggests that in situations where $\dim(\operatorname{Ker}\mathbf{J}_0) = 1$, the Fredholm alternative is equivalent to normalizing the OTD series expansion. In the next example, we illustrate application of the Fredholm alternative in computation of the OTD manifold for a low-dimensional nonlinear system.

4.3.2. Unsteady nonlinear dynamics. We consider a classic model for enzyme kinetics, the Michaelis–Menten equations,

$$\varepsilon\dot{x} = y - (y+\kappa)x, \tag{4.32a}$$

$$\dot{y} = -y + (y + \kappa - \lambda)x, \tag{4.32b}$$

where κ and λ are bounded, positive constants, and the state variables x and y represent nondimensional chemical concentrations. As discussed in [30], this system exhibits general phenomena commonly found in singularly perturbed systems. In particular, the linearized operator associated with the vector field (4.32a) and (4.32b) is unsteady and nonnormal, leading to significant transient growth of the solution. This is illustrated in Figure 1, where we show time series for x and y computed using a third-order Adams–Bashforth integrator with time-step size $\Delta t = 10^{-2}$, initial conditions $\mathbf{z}_0 = \begin{bmatrix}0.01 & 1\end{bmatrix}^T$, and parameters $\varepsilon = 0.1$, $\lambda = 0.5$, and $\kappa = 1$. We also note that the system admits a normally hyperbolic limiting invariant manifold

$$\mathcal{W}_0 = \left\{(x,y)\,|\,x = \frac{y}{y+\kappa}\right\} \tag{4.33}$$

when $\varepsilon = 0$, and a locally stable SIM

$$\mathcal{W}_\varepsilon = \left\{(x,y)\,|\,x = \frac{y}{y+\kappa} + \varepsilon\frac{\lambda\kappa y}{(y+\kappa)^4} + \mathcal{O}(\varepsilon^2)\right\} \tag{4.34}$$

when $0 < \varepsilon \ll 1$ [30].

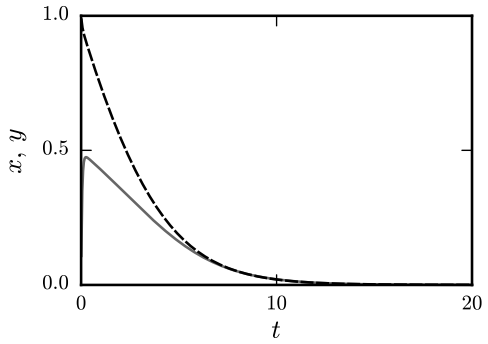

Figure 1. *Time series of x (solid grey) and y (dashed black) for the Michaelis–Menten equations with parameters $\varepsilon = 0.1$, $\lambda = 0.5$, and $\kappa = 1$, and initial conditions $x(0) = 0.01$ and $y(0) = 1$.*

The limiting OTD manifold is found by solving $(\mathbf{I} - \mathbf{u}^{(0)}\mathbf{u}^{(0)T})\mathbf{J}_0\mathbf{u}^{(0)} = \mathbf{0}$, leading to two solutions,

$$\mathbf{u}^{(0)} = \begin{bmatrix} 1 & 0 \end{bmatrix}^T \in (\operatorname{Ker}\mathbf{J}_0)^{\mathrm{c}}, \tag{4.35a}$$

$$\mathbf{u}^{(0)} = \begin{bmatrix} \alpha(x,y)(1-x) & \alpha(x,y)(\kappa+y) \end{bmatrix}^T \in \operatorname{Ker}\mathbf{J}_0, \tag{4.35b}$$

where $\alpha(x, y)$ is a factor yet to be determined. For $\mathbf{u}^{(0)} \in (\operatorname{Ker}\mathbf{J}_0)^{\mathrm{c}}$, the $\mathcal{O}(\varepsilon)$ subproblem is well posed and gives a unique solution,

$$\mathbf{u}^{(1)} = \begin{bmatrix} 0 & -\dfrac{\kappa - \lambda + y}{\kappa + y} \end{bmatrix}^T. \tag{4.36}$$

This solution corresponds to the least unstable direction, and is of little interest to us. We therefore turn to (4.35b), for which the factor $\alpha(x, y)$ remains to be found. As discussed earlier, it is straightforward to argue that α is nothing more than a normalization factor. However, we will play along and blindly apply the recipe given in subsection 4.1; that is, we determine α with the Fredholm alternative. We first construct a basis of $\operatorname{Ker}(\mathbf{I}-\mathbf{u}^{(0)}\mathbf{u}^{(0)T})\mathbf{J}_0$. Let $\mathbf{s}_0 = \begin{bmatrix} 1-x & \kappa+y \end{bmatrix}^T$ be such a basis vector. The Fredholm alternative then requires that

$$\langle \mathbf{s}_0, \nabla\mathbf{u}^{(0)}\,\mathbf{h}_1(\mathbf{x},\mathbf{y}) - (\mathbf{I} - \mathbf{u}^{(0)}\mathbf{u}^{(0)T})\mathbf{J}_1\mathbf{u}^{(0)} \rangle = 0, \tag{4.37}$$

leading to

$$\begin{aligned} &\frac{\partial\alpha}{\partial y}\left[(1-x)^2 + (y+\kappa)^2\right] + (y+\kappa)\alpha \\ &\quad + \alpha\frac{\lambda(1-x)(y+\kappa)}{(y+\kappa-\lambda)x - y}\left\{\alpha^2\left[(1-x)^2 + (y+\kappa)^2\right] - 1\right\} = 0. \end{aligned} \tag{4.38}$$

Hence, we have

$$\alpha = \frac{1}{\sqrt{(1-x)^2 + (y+\kappa)^2}}, \tag{4.39}$$

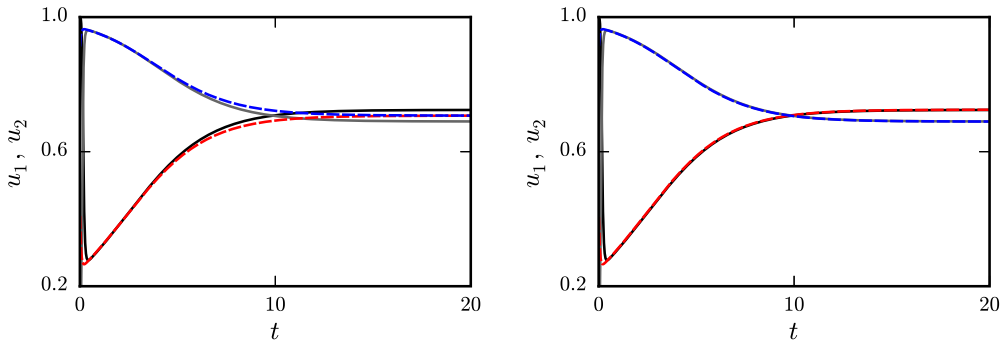

Figure 2. *Time series for the two coordinates of the first OTD mode corresponding to the trajectory in Figure 1:* (a) *zeroth-order approximation (dashed blue and dashed red) compared to numerical integration (solid grey and solid black), and* (b) *first-order approximation (dashed blue and dashed red) compared to numerical integration (solid grey and solid black).*

which corresponds to the expected normalization factor. Now that $\mathbf{u}^{(0)}$ has been fully determined, we may proceed to the next order of approximation. The $\mathcal{O}(\varepsilon)$ subproblem likewise gives a line of solutions. The undetermined factor is found by invoking the Fredholm alternative in the $\mathcal{O}(\varepsilon^2)$ subproblem. We obtain a unique solution for $\mathbf{u}^{(1)}$, and write the OTD mode as

$$\begin{aligned}\mathbf{u} = &\frac{1}{\sqrt{(1-x)^2+(\kappa+y)^2}}\begin{bmatrix}1-x & \kappa+y\end{bmatrix}^T \\ &-\varepsilon\frac{(x-1)[\lambda+\kappa x-2\lambda x+y(x-1)]}{[(1-x)^2+(\kappa+y)^2]^{3/2}}\begin{bmatrix}1 & \dfrac{x-1}{\kappa+y}\end{bmatrix}^T+\mathcal{O}(\varepsilon^2).\end{aligned} \tag{4.40}$$

The above is a representation of the first OTD mode as a function of the state variables only; that is, a graph from the physical space to the OTD space in which the history of the trajectory and the initial conditions do not appear. Such a representation allows for immediate identification of the most unstable direction in the phase space with no need for time integration of the governing equations.

Figure 2 shows a comparison between the zeroth-order and first-order asymptotic approximations of the OTD mode (4.40), and numerical integration of (4.12) with initial conditions $u_1(0)=1$ and $u_2(0)=0$. (The zeroth-order and first-order approximations of the OTD mode are defined as $\mathbf{u}^{(0)}$ and $\mathbf{u}^{(0)}+\varepsilon\mathbf{u}^{(1)}$, respectively.) Good agreement is found between the analysis and the numerics, even to leading order. In particular, the SIM approach captures the early episode of nonnormal growth. We note that such good agreement (modulo a sign difference) has been found irrespective of the initial conditions selected for integration of (4.12). We also note that at long times, the OTD mode behaves as

$$\lim_{t\to+\infty}\mathbf{u}=\frac{1}{\sqrt{1+\kappa^2}}\begin{bmatrix}1\\ \kappa\end{bmatrix}+\varepsilon\frac{\lambda\kappa}{(1+\kappa^2)^{3/2}}\begin{bmatrix}\kappa\\ -1\end{bmatrix}+\mathcal{O}(\varepsilon^2), \tag{4.41}$$

which coincides with the most unstable (normalized) eigenvector of the linearized operator evaluated at the fixed point $x = y = 0$.

5. Extension to general dynamical systems without explicit time-scale separation. The approach presented in section 4 assumes that slow-fast separation of time scales appears explicitly in the equations of motion in the form of a small parameter ε. However, numerous dynamical systems exhibit slow-fast dynamics despite no small parameter being present in the governing equations. So it would be valuable to extend the approach in section 4 to situations in which slow-fast dynamics are seen, although no small parameter is available from the equations of motion. The objective is to find a similar mapping from physical space to OTD space that would allow for prediction and possibly control of transient instabilities without any knowledge of the history of the trajectory.

5.1. Methodology. We return to (2.1), and first note that recurring transient instabilities are associated with the presence of multiple time scales that are well apart from one another. It is thus natural to introduce a fast time scale, $\hat{t} = t/\nu$, corresponding to the time scale at which transient bursts occur. Here, ν is a small parameter ($0 < \nu \ll 1$) that can be estimated by examining the time series of some observable, but remains otherwise inaccessible. (In particular, ν does not appear explicitly in the governing equations.) At this time scale, the trajectory is governed by

$$\nu \mathbf{z}^\dagger = \mathbf{F}(\mathbf{z}), \tag{5.1a}$$

and the first OTD mode by

$$\nu \mathbf{u}^\dagger = \big(\mathbf{I} - \mathbf{u}\mathbf{u}^T\big)\mathbf{L}\mathbf{u}, \tag{5.1b}$$

where the dagger denotes differentiation with respect to $\hat{t}$.

The OTD equation (5.1b) lends itself to singular perturbation theory. Assuming that $\nu \ll 1$ (that is, bursting episodes are sufficiently pronounced), we expand $\mathbf{u}$ as a power series in ν, $\mathbf{u} = \mathbf{u}^{(0)} + \nu\mathbf{u}^{(1)} + \cdots$. We emphasize that this expansion is valid (i.e., uniformly convergent in ν) only in those time intervals during which an extreme event occurs. Hence, we do not expect our approximate solution to agree with the numerical solution of (2.6) in intervals during which no strong instability is seen.

Substituting the expansion in (5.1b) and equating terms of equal powers of ν leads to a hierarchy of subproblems, the first two of which are given by

$$(\mathbf{I} - \mathbf{u}^{(0)}\mathbf{u}^{(0)T})\mathbf{L}\mathbf{u}^{(0)} = \mathbf{0}, \tag{5.2a}$$

$$\nabla_{\mathbf{z}}\mathbf{u}^{(0)}\,\mathbf{F} = (\mathbf{I} - \mathbf{u}^{(0)}\mathbf{u}^{(0)T})\mathbf{L}\mathbf{u}^{(1)} - (\mathbf{u}^{(1)}\mathbf{u}^{(0)T} + \mathbf{u}^{(0)}\mathbf{u}^{(1)T})\mathbf{L}\mathbf{u}^{(0)}, \tag{5.2b}$$

at $\mathcal{O}(1)$ and $\mathcal{O}(\nu)$, respectively. The above are similar to their respective counterparts (4.18) and (4.20) found for slow-fast systems in section 4. In particular, the algebraic nature of the $\mathcal{O}(1)$ subproblem shows that $\mathbf{u}^{(0)}$ can be expressed as a graph over the state $\mathbf{z}$. The $\mathcal{O}(\nu)$ subproblem is linear in $\mathbf{u}^{(1)}$, which means that $\mathbf{u}^{(1)}$ can likewise be expressed as a function of $\mathbf{z}$ only. (It is straightforward to show that this holds for all higher-order subproblems.) One notable difference, however, is that the linearized operator $\mathbf{L}$ generally has full rank, as

opposed to $\mathbf{J}_0$ which had a nontrivial kernel. The $\mathcal{O}(\nu^k)$ subproblems ($k > 0$) thus do not require invoking the Fredholm alternative as they all admit a unique solution.

We note that in practice, it is convenient to solve for $\nu\mathbf{u}^{(1)}$ as opposed to $\mathbf{u}^{(1)}$ in (5.2). This is because the term on the left-hand side of (5.2) then becomes $\nu\mathbf{u}^{(0)\dagger}$. The latter can be computed directly by solving (5.2) at two consecutive time instants t and $t+\delta t$, and proceeding in the limit $\delta t \to 0$. (In discrete time, one can solve (5.2) at several consecutive time steps, and approximate $\nu\mathbf{u}^{(0)\dagger}$ with any suitable discretization formula.) The advantage of this method is that the power series expansion for $\mathbf{u}$ can be computed without ever assigning a value to ν.

5.2. Application to the Charney–DeVore equations. We apply the manifold approach proposed in subsection 5.1 to a modified version of the classic Charney–DeVore model [11], which describes atmospheric circulations at midlatitudes. We consider a six-dimensional truncation of the original system, which models barotropic flow in a plane channel with topography [13, 3]. The governing equations are given by

$$\dot{z}_1 = \gamma_1^* z_3 - C(z_1 - z_1^*), \tag{5.3a}$$

$$\dot{z}_2 = -(\alpha_1 z_1 - \beta_1) z_3 - C z_2 - \delta_1 z_4 z_6, \tag{5.3b}$$

$$\dot{z}_3 = (\alpha_1 z_1 - \beta_1) z_2 - \gamma_1 z_1 - C z_3 + \delta_1 z_4 z_5, \tag{5.3c}$$

$$\dot{z}_4 = \gamma_2^* z_6 - C(z_4 - z_4^*) + \mu(z_2 z_6 - z_3 z_5), \tag{5.3d}$$

$$\dot{z}_5 = -(\alpha_2 z_1 - \beta_2) z_6 - C z_5 - \delta_2 z_4 z_3, \tag{5.3e}$$

$$\dot{z}_6 = (\alpha_2 z_1 - \beta_2) z_5 - \gamma_2 z_4 - C z_6 + \delta_2 z_4 z_2. \tag{5.3f}$$

The model parameters are given by $\alpha_m = 8\sqrt{2}m^2(b^2 + m^2 - 1)/[\pi(4m^2 - 1)(b^2 + m^2)]$ and $\delta_m = 64\sqrt{2}(b^2 - m^2 + 1)/[15\pi(b^2 + m^2)]$, representing zonal advection in the z_1 and z_4 directions, respectively; $\beta_m = \beta b^2/(b^2 + m^2)$, representing the so-called β effects; $\gamma_m = 4\sqrt{2}m^3\gamma b/[\pi(4m^2 - 1)(b^2 + m^2)]$ and $\gamma_m^* = 4\sqrt{2}m\gamma b/[\pi(4m^2 - 1)]$, representing topographic interactions; and $\mu = 16\sqrt{2}/(5\pi)$. (Here, $m = 1$ or 2.) The parameters C, z_1^*, and z_4^* account for Ekman damping, zonal forcing in the z_1 direction, and zonal forcing in the z_4 direction, respectively. We set $z_1^* = 0.95$, $z_4^* = -0.76095$, $C = 0.1$, $\beta = 1.25$, $\gamma = 0.2$, and $b = 0.5$. As discussed in [13, 3], these values of the parameters give rise to significant transitions between "zonal" and "blocked" flow regimes, resulting from a nonlinear interaction between barotropic and topographic instabilities. These severe transitions are the manifestation of significant time-scale separation, despite the fact that there is no explicit small parameter in (5.3a)–(5.3f). Equations (5.3a)–(5.3f) are integrated using a third-order Adams–Bashforth scheme with time-step size $\Delta t = 10^{-3}$, and zero initial conditions, except for $z_1(0) = 1.14$ and $z_4(0) = -0.91$.

Figure 3 shows time series for the six coordinates of the trajectory, with several clear transitions between zonal and blocked regimes. The intervals of blocked flow (e.g., $725 \le t \le 980$ and $1575 \le t \le 1804$) are associated with transient instabilities, and are of main interest to us. It is in those intervals that we assess the accuracy of our asymptotic expansion. For the regime transition occurring in the interval $725 \le t \le 980$, Figure 4 shows the first OTD mode computed by numerically integrating (2.6), along with its zeroth- and first-order approximations computed with the approach described in subsection 5.1. We note that the leading-order

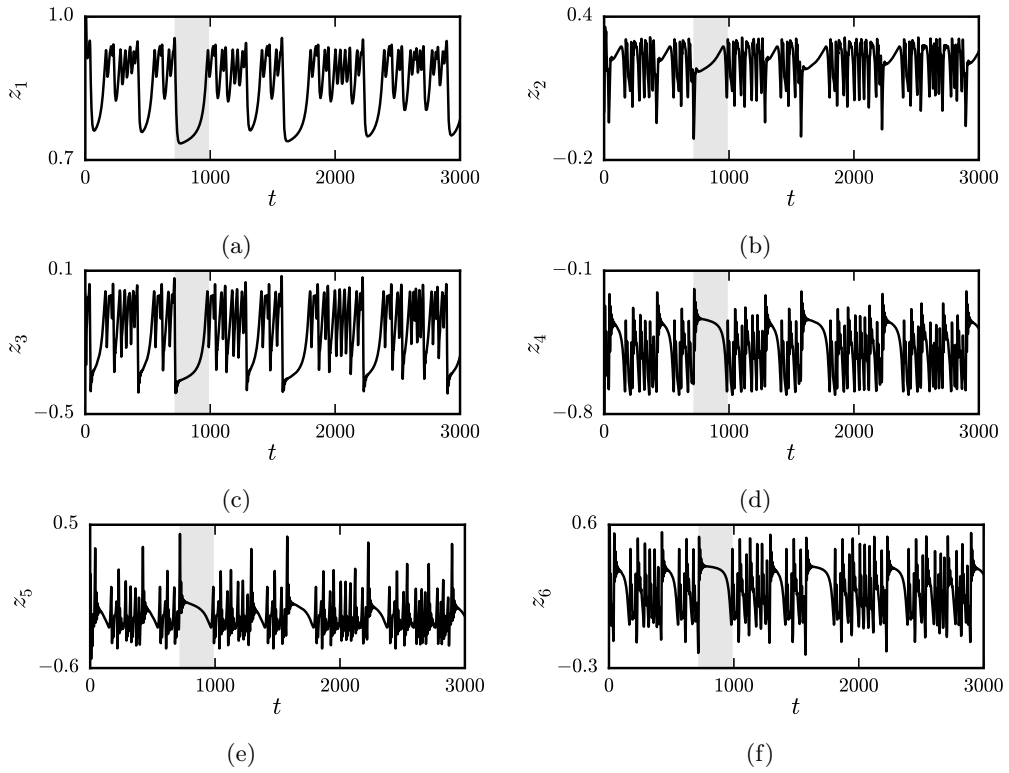

Figure 3. *Time series for the six-dimensional Charney–DeVore model with parameters and initial conditions given in the text. The shaded interval* $725 \leq t \leq 980$ *corresponds to a regime of blocked flow.*

term $\mathbf{u}^{(0)}$ is already a good approximation to $\mathbf{u}$, and the first-order term $\nu\mathbf{u}^{(1)}$ merely adds small corrections to $\mathbf{u}^{(0)}$. We also note that our approximation performs poorly outside the regime of interest, as anticipated.

6. Conclusions. The present work focused on prediction of transient instabilities in finite-dimensional dynamical systems. We considered a recently introduced framework, the OTD modes, consisting of an evolving reduced-order set of orthonormal vectors that had been shown to track the most unstable directions along a given trajectory. Although it had become clear that the OTD modes could be used to characterize transient instabilities at relatively low computational cost, little had been known about their intrinsic properties and how they relate to other existing techniques, such as covariant Lyapunov vectors, GS vectors, or singular vectors, which, too, claim to quantify stable and unstable directions in tangent space. One of the main contributions of the present paper is a proof of equivalence between the OTD modes and the GS vectors when the latter are continuously orthonormalized along the trajectory. This important result established a link between OTD modes and covariant Lyapunov vectors and, perhaps more importantly, implied that the OTD modes, at long times, converge to a well-defined basis that depends only on the state of the system in the phase space and not on the history of the trajectory prior to reaching the attractor. This feature had long been surmised based on numerical evidence in previous studies (it was even rigorously proven in

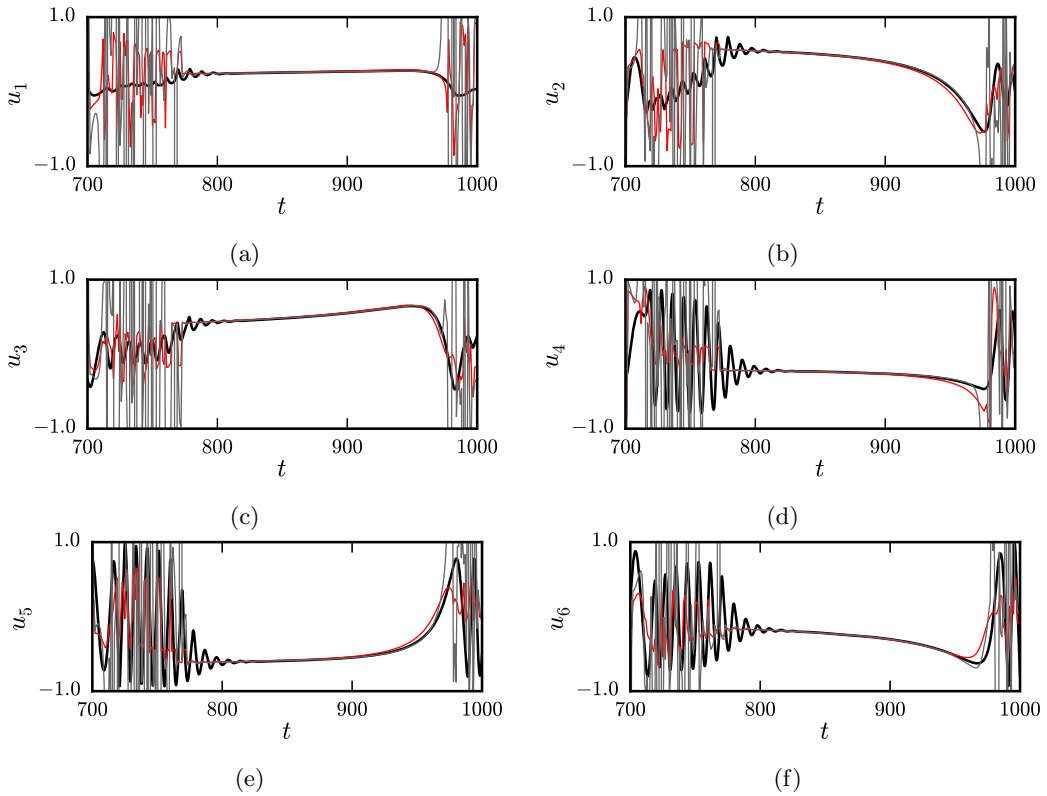

Figure 4. *Detail of the coordinates of the first OTD mode in an interval including the regime of blocked flow highlighted in Figure 3 (black: numerical integration; red: zeroth-order approximation; grey: first-order approximation).*

the special case of hyperbolic fixed points). The equivalence between GS vectors and OTD modes provided a definitive answer to the question.

The fact that the OTD modes converge to a set of vectors defined at every point of the attractor called for developing approximate solutions of the OTD modes, very much like those based on invariant manifold theory in slow-fast systems. We considered a generic finite-dimensional slow-fast system in which time-scale separation appeared explicitly in the equations of motion in the form of a small parameter ε. Assuming that the trajectory of the system was attracted to a slow manifold (with transient instabilities and growth of the fast variables occurring along the unstable manifold of the slow manifold), we proposed an analytical description of the OTD modes that took the form of an asymptotic expansion in terms of ε. We obtained a map from the phase space (or, equivalently, the slow manifold of the trajectory) to the OTD space, thus providing approximations for the directions of instability at every point in the phase space. We then extended the method to systems in which clear transient instabilities arise despite the fact that no small parameter appears in the governing equations. In both situations, we found good agreement between the analytical approach and the numerical solutions.

The present results strongly suggest that the proposed analytical formulation could be applied to more complex dynamical systems with a view to mitigating transient instabilities. A particularly attractive feature of the manifold approach is that it requires solving a limited number of algebraic equations (with no more than one being nonlinear), possibly at selected points along the trajectory, as opposed to solving multiple initial-value problems to obtain the temporal evolution of each OTD mode. This points to the possibility of using the OTD manifold framework to identify directions responsible for transient instability at any given point along a trajectory, and to design a controller that acts locally in the phase space (independently of the history of the trajectory) in order to suppress those instabilities.

Acknowledgments. The authors gratefully acknowledge insightful discussions with Dr. Mohammad Farazmand and Mr. Saviz Mowlavi.

REFERENCES

[1] N. Akhmediev, J. M. Dudley, D. R. Solli, and S. K. Turitsyn, *Recent progress in investigating optical rogue waves*, J. Opt., 15 (2013), 060201.
[2] S. Albeverio, V. Jentsch, and H. Kantz, *Extreme Events in Nature and Society*, Springer, New York, 2006.
[3] H. Babaee, M. Farazmand, G. Haller, and T. P. Sapsis, *Reduced-order description of transient instabilities and computation of finite-time Lyapunov exponents*, Chaos, 27 (2017), 063103.
[4] H. Babaee and T. P. Sapsis, *A minimization principle for the description of modes associated with finite-time instabilities*, R. Soc. Proc. A Math. Phys. Eng. Sci., 472 (2016), 20150779.
[5] G. Benettin, L. Galgani, A. Giorgilli, and J.-M. Strelcyn, *Lyapunov characteristic exponents for smooth dynamical systems and for Hamiltonian systems; A method for computing all of them. Part 1: Theory*, Meccanica, 15 (1980), pp. 9–20.
[6] G. Benettin, L. Galgani, and J.-M. Strelcyn, *Kolmogorov entropy and numerical experiments*, Phys. Rev. A (3), 14 (1976), pp. 2338–2345.
[7] H. Bosetti and H. A. Posch, *Covariant Lyapunov vectors for rigid disk systems*, Chem. Phys., 375 (2010), pp. 296–308.
[8] H. Bosetti, H. A. Posch, C. Dellago, and W. G. Hoover, *Time-reversal symmetry and covariant Lyapunov vectors for simple particle models in and out of thermal equilibrium*, Phys. Rev. E (3), 82 (2010), 046218.
[9] W. Cai, S. Borlace, M. Lengaigne, P. Van Rensch, M. Collins, G. Vecchi, A. Timmermann, A. Santoso, M. J. McPhaden, L. Wu, M. H. England, G. Wang, E. Guilyardi, and J. Fei-Fei, *Increasing frequency of extreme El Niño events due to greenhouse warming*, Nature Climate Change, 4 (2014), pp. 111–116.
[10] J. Carr, *Applications of Centre Manifold Theory*, Springer, New York, 1981.
[11] J. G. Charney and J. G. DeVore, *Multiple flow equilibria in the atmosphere and blocking*, J. Atmos. Sci., 36 (1979), pp. 1205–1216.
[12] W. Cousins and T. P. Sapsis, *Quantification and prediction of extreme events in a one-dimensional nonlinear dispersive wave model*, Phys. D, 280 (2014), pp. 48–58.
[13] D. T. Crommelin, J. D. Opsteegh, and F. Verhulst, *A mechanism for atmospheric regime behavior*, J. Atmos. Sci., 61 (2004), pp. 1406–1419.
[14] K. Dysthe, H. E. Krogstad, and P. Müller, *Oceanic rogue waves*, Annu. Rev. Fluid Mech., 40 (2008), pp. 287–310.
[15] S. V. Ershov and A. B. Potapov, *On the concept of stationary Lyapunov basis*, Phys. D, 118 (1998), pp. 167–198.
[16] M. Farazmand and T. P. Sapsis, *Dynamical indicators for the prediction of bursting phenomena in high-dimensional systems*, Phys. Rev. E (3), 94 (2016), 032212.
[17] N. Fenichel, *Geometric singular perturbation theory for ordinary differential equations*, J. Differential Equations, 31 (1979), pp. 53–98.

[18] N. Fenichel and J. K. Moser, *Persistence and smoothness of invariant manifolds for flows*, Indiana Univ. Math. J., 21 (1971), pp. 193–226.
[19] U. Frisch, *Fully developed turbulence and intermittency*, Ann. New York Acad. Sci., 357 (1980), pp. 359–367.
[20] F. Ginelli, H. Chaté, R. Livi, and A. Politi, *Covariant Lyapunov vectors*, J. Phys. A, 46 (2013), 254005.
[21] F. Ginelli, P. Poggi, A. Turchi, H. Chaté, R. Livi, and A. Politi, *Characterizing dynamics with covariant Lyapunov vectors*, Phys. Rev. Lett., 99 (2007), 130601.
[22] I. Goldhirsch, P.-L. Sulem, and S. A. Orszag, *Stability and Lyapunov stability of dynamical systems: A differential approach and a numerical method*, Phys. D, 27 (1987), pp. 311–337.
[23] J. R. Green, A. B. Costa, B. A. Grzybowski, and I. Szleifer, *Relationship between dynamical entropy and energy dissipation far from thermodynamic equilibrium*, Proc. Natl. Acad. Sci. USA, 110 (2013), pp. 16339–16343.
[24] W. G. Hoover and C. G. Hoover, *Local Gram–Schmidt and covariant Lyapunov vectors and exponents for three harmonic oscillator problems*, Commun. Nonlinear Sci. Numer. Simul., 17 (2012), pp. 1043–1054.
[25] W. G. Hoover, H. A. Posch, and S. Bestiale, *Dense-fluid Lyapunov spectra via constrained molecular dynamics*, J. Chem. Phys., 87 (1987), pp. 6665–6670.
[26] P. V. Kuptsov and U. Parlitz, *Theory and computation of covariant Lyapunov vectors*, J. Nonlinear Sci., 22 (2012), pp. 727–762.
[27] G. Lapeyre, *Characterization of finite-time Lyapunov exponents and vectors in two-dimensional turbulence*, Chaos, 12 (2002), pp. 688–698.
[28] B. Legras and R. Vautard, *A guide to Liapunov vectors*, in Predictability, Vol. 1, European Centre for Medium-Range Weather Forecasts, Reading, England, 1996, pp. 135–146.
[29] A. J. Majda and Y. Lee, *Conceptual dynamical models for turbulence*, Proc. Natl. Acad. Sci. USA, 111 (2014), pp. 6548–6553.
[30] R. E. J. O'Malley, *Singular Perturbation Methods for Ordinary Differential Equations*, Springer, New York, 1991.
[31] R. D. Peters, M. Le Berre, and Y. Pomeau, *Prediction of catastrophes: An experimental model*, Phys. Rev. E (3), 86 (2012), 026207.
[32] H. A. Posch and W. G. Hoover, *Lyapunov instability of dense Lennard–Jones fluids*, Phys. Rev. A (3), 38 (1988), 473.
[33] K. Sakamoto, *Invariant manifolds in singular perturbation problems for ordinary differential equations*, Proc. Roy. Soc. Edinburgh Sect. A, 116 (1990), pp. 45–78.
[34] T. P. Sapsis and P. F. J. Lermusiaux, *Dynamically orthogonal field equations for continuous stochastic dynamical systems*, Phys. D, 238 (2009), pp. 2347–2360.
[35] I. Shimada and T. Nagashima, *A numerical approach to ergodic problem of dissipative dynamical systems*, Prog. Theor. Phys., 61 (1979), pp. 1605–1616.
[36] D. R. Solli, C. Ropers, P. Koonath, and B. Jalali, *Optical rogue waves*, Nature, 450 (2007), pp. 1054–1057.
[37] Z. Toth and E. Kalnay, *Ensemble forecasting at NMC: The generation of perturbations*, Bull. Amer. Meteorol. Soc., 74 (1993), pp. 2317–2330.
[38] W. E. Wiesel, *Continuous time algorithm for Lyapunov exponents*. I, Phys. Rev. E (3), 47 (1993), pp. 3686–3691.
[39] A. Wolf, J. B. Swift, H. L. Swinney, and J. A. Vastano, *Determining Lyapunov exponents from a time series*, Phys. D, 16 (1985), pp. 285–317.
[40] H.-L. Yang and G. Radons, *Comparison between covariant and orthogonal Lyapunov vectors*, Phys. Rev. E (3), 82 (2010), 046204.